PROGRESS IN COLOR, COLORANTS AND COATINGS

available online @ www.pccc.icrc.ac.ir

Progress in Color Colorants Coating 17 (2024), 1-10

Ministry of Science, Research and Technology
Institute for Color Science & Technology

Evaluation of 2-Dimethylaminopropionamidoantipyrine as a Corrosion Inhibitor for Mild Steel in HCl Solution: A Combined Experimental and Theoretical Study

M.K. Abbass[1], K.M. Raheef[2], I.A. Aziz[1], M.M. Hanoon[1], A.M. Mustafa[1], W.K. Al-Azzawi[3], A.A. Al-Amiery[4,5*], A.A.H. Kadhum[6]

1. Department of Production Engineering and Metallurgy, University of Technology, P.O. Box: 10001Baghdad, Iraq
2. Ashur University College, P.O. Box: 10001, Baghdad, Iraq
3. Al-Farahidi University, P.O. Box: 10001, Baghdad, Iraq
4. Energy and Renewable Energies Technology Center, University of Technology, Iraq, P.O. Box: 10001Baghdad, Iraq
5. Faculty of Engineering and Built Environment, Universiti Kebangsaan Malaysia, Bangi, P.O. Box: 43600, Selangor, Malaysia
6. Dijla University College, P.O. Box: 10001, Baghdad, Iraq

ARTICLE INFO

Article history:
Received: 26 Apr 2023
Final Revised: 20 June 2023
Accepted: 25 June 2023
Available online: 11 Oct 2023

Keywords:
Corrosion inhibition
2-Dimethylaminopropionamido antipyrine (DMAPAAP)
Mild steel
Hydrochloric acid (HCl)
Density functional theory (DFT)

ABSTRACT

A combined experimental and theoretical study investigated the corrosion inhibition potential of 2-dimethylaminopropionamidoanti-pyrine (DMAPAAP) on mild steel in 1 M hydrochloric acid (HCl) solution. The weight loss method was used to determine the corrosion rate of mild steel in HCl solution both in the absence and presence of different concentrations of DMAPAAP. The effect of exposure time and temperature on the corrosion inhibition efficiency of DMAPAAP was also investigated. The results showed that DMAPAAP exhibited good inhibitory properties against the corrosion of mild steel in an HCl solution. The corrosion rate of mild steel increased with increasing inhibitor concentration, exposure time, and temperature. The highest inhibition efficiency of 91.9 % was achieved at 5 mM concentration of DMAPAAP after 5 hours of exposure time at 333 K. Density functional theory (DFT) calculations were carried out to support the experimental results and understand the inhibition process's mechanism. The adsorption of DMAPAAP on the mild steel surface was found to be both chemisorption and physisorption and followed the Langmuir adsorption isotherm. The inhibition efficiency increased with increasing electron-donating groups in the molecule, which was attributed to forming a protective film on the metal surface. Overall, the combined experimental and theoretical study provides a deeper understanding of the corrosion inhibition mechanism of DMAPAAP on mild steel in HCl solution and demonstrates its potential as an effective corrosion inhibitor for mild steel in industrial applications. Prog. Color Colorants Coat. 17 (2024), 1-10© Institute for Color Science and Technology.

1. Introduction

Corrosion is a natural process in many industries and causes significant economic losses and safety and environmental hazards [1, 2]. One material that is particularly susceptible to corrosion is mild steel. In industries such as oil and gas, mild steel is widely used for its good mechanical properties and low cost. However, acidic solutions like hydrochloric acid (HCl)

*Corresponding author: * dr.ahmed1975@ukm.edu.my
dr.ahmed1975@gmail.com

Doi: 10.30509/pccc.2023.167081.1197

can lead to severe, mild steel corrosion, limiting practical applications. Therefore, developing effective corrosion inhibitors for mild steel in acidic environments has become an important research area in materials science [3, 4]. The problem of corrosion of mild steel in acidic solutions, such as HCl, has been a major concern in many industries, especially in the oil and gas industry [5]. The presence of HCl in oil and gas production can cause significant corrosion of mild steel equipment and pipelines, resulting in equipment failure, leaks, and environmental contamination. In addition, using strong acids like HCl for cleaning and descaling operations can also lead to the corrosion of mild steel surfaces [6, 7]. To address this problem, many researchers have focused on developing effective corrosion inhibitors for mild steel in acidic environments [8]. In recent years, organic corrosion inhibitors have gained increasing attention due to their relative safety, environmental friendliness, and cost-effectiveness compared to traditional inorganic inhibitors [9]. These organic inhibitors can form a protective film on the metal surface, which prevents the corrosive species from attacking the metal and reduces the corrosion rate [10-17]. Several organic inhibitors have been studied for their potential to inhibit mild steel corrosion in acidic solutions. For example, heterocyclic compounds containing nitrogen, oxygen, or sulfur atoms in their structures have been found to exhibit good inhibitory properties [18-21]. Antipyrine derivatives have shown promising inhibitory properties against mild steel corrosion in acidic solutions. Antipyrine derivatives can form complexes with metal ions and create a protective layer on the metal surface, which reduces the corrosion rate. Antipyrine derivatives are a class of heterocyclic compounds reported to exhibit good inhibitory properties against corrosion in acidic environments. For instance, N-substituted antipyrines, such as N-phenyl and N-methyl derivatives, are effective inhibitors for mild steel corrosion in HCl solution due to their ability to form complexes with metal ions and to create a protective layer on the metal surface [21, 22].

In addition to experimental studies, computational methods, such as DFT calculations, have also been used to investigate the inhibitory mechanism of organic compounds on metal corrosion. DFT calculations can provide insights into the electronic structure and adsorption behavior of inhibitors on metal surfaces, which can aid in designing and optimizing new corrosion inhibitors [23, 24].

In summary, developing effective and environmentally friendly corrosion inhibitors for mild steel in acidic solutions is very important. DMAPAAP, a new type of antipyrine derivative, has shown promising inhibitory properties and warrants further investigation using experimental and theoretical methods. In this study, the inhibitory properties of DMAPAAP on the corrosion of mild steel in an HCl solution were investigated using experimental and theoretical methods. The weight loss method was used to evaluate the corrosion rate of mild steel in the absence and presence of DMAPAAP at different concentrations, exposure times, and temperatures. Density functional theory (DFT) calculations were also performed to elucidate the inhibition mechanism and provide insights into the adsorption behavior of DMAPAAP (Figure 1) on the mild steel surface.

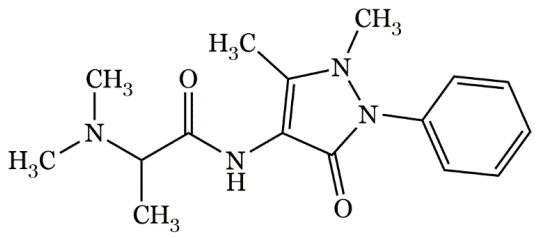

Figure 1: The chemical structure of DMAPAAP.

2. Experimental

All chemicals were of analytical grade purity and were procured from reputable suppliers.

2.1. Weight loss measurements

In the present study, X-ray fluorescence spectrometry was used to determine the chemical composition of the mild steel samples. The samples were prepared according to ASTM G1-03 [25] and polished using silicon carbide series plates. Before immersion, the mild steel coupons were rinsed in double-distilled water and acetone and dried in an oven. To simulate the corrosive media used in the experiments, 1 M HCl solution was prepared by diluting analytical grade 37 % HCl solution with double-distilled water. The inhibitor concentrations (0.1, 0.2, 0.3, 0.4, 0.5, and 1.0 mM) were obtained by diluting the inhibitor in 1 M HCl solution. The mild steel samples were weighed and immersed in 500 mL glass beakers containing 400 mL of 1 M HCl solution without and with different

inhibitor concentrations. The experiments were performed at 303 K using a water bath following NACE TM0169/G31 [26]. The samples were exposed for various periods (1, 5, 10, 24, and 48 hours), and the corrosion products were wiped off the surface before drying and weighing the coupons. The difference in weight was documented, and the mass variation at the estimated time and original mass of the metallic sample represented the weight loss that was attained [27]. To determine the effect of temperature, mild steel coupons were immersed in corrosive media (1 M HCl) containing different concentrations of the inhibitor (0.1, 0.2, 0.3, 0.4, 0.5, and 1 mM) at 303, 313, 323, and 333 K using a water bath. The average corrosion rate was calculated after exposure in triplicate, and the corrosion rate was calculated using equation 1 [28].

$$C_R = \frac{W}{adt} \quad (1)$$

The inhibition efficiency can be calculated using equation 2, where W represents the weight loss (mg) of the tested sample; a denotes the surface area of mild steel (cm^2); d refers to the density of the mild steel coupon (g/cm^3), and t represents the exposure time (h) [29].

$$IE\% = [1 - \frac{C_{R(i)}}{C_{R_o}}] \times 100 \quad (2)$$

The rates of corrosion in uninhibited and inhibited solutions were denoted as C_{R_o} and $C_{R(i)}$, respectively. The coverage area (θ) for both uninhibited and inhibited solutions was determined using equation 3 [30].

$$\theta = 1 - \frac{C_{R(i)}}{C_{R_o}} \quad (3)$$

2.2. Adsorption model

To obtain more information about the properties of the investigated molecules, it is important to use different types of adsorption isotherms such as Frumkin, Temkin, and Langmuir. By using these isotherms, the degree of surface coverage of the inhibitor can be determined. Hence, in the present study, the degree of surface coverage of the inhibitor was determined for various concentrations in corrosive media using weight loss measurements [31].

2.3. Theoretical calculations

The quantum chemical calculations were performed using Gaussian 09 software [16]. The optimization of the inhibitor structure in the gaseous state was carried out using the B3LYP method and the basis set "6-$31G^{++}$ (d,p)". The ionization potential (I) and electron affinity (A) were determined based on Koopmans theory [32], where I is related to E_{HOMO} and A is related to E_{LOMO}. Equations 4 and 5 were used to determine I and A.

$$I = -E_{HOMO} \quad (4)$$

$$A = -E_{LOMO} \quad (5)$$

The electronegativity (χ), hardness (η), and softness (σ) were determined using equations 6-8.

$$\chi = \frac{I+A}{2} \quad (6)$$

$$\eta = \frac{I-A}{2} \quad (7)$$

$$\sigma = \eta^{-1} \quad (8)$$

To calculate the number of electrons transferred (ΔN), Equation 9 from [33] was employed.

$$\Delta N = \frac{\chi_{Fe} - \chi_{inh}}{2(\eta_{Fe} + \eta_{inh})} \quad (9)$$

The electronegativity of iron was determined to be 7 eV, while its hardness value was found to be zero eV. These results were used to develop equation 10.

$$\Delta N = \frac{7 - \chi_{inh}}{2(\eta_{inh})} \quad (10)$$

3. Result and Discussion

3.1. Effect of concentration

The weight loss measurements were used to examine the corrosion performance of mild steel samples in a 1 M corrosive environment, with and without the addition of various doses of DMAPAAP, after 5 hours of immersion time at 303 K. Figure 2 presents the rate of corrosion and inhibition effectiveness. The figure indicates that the inhibitor's ability to prevent corrosion increases with a concentration of up to 0.5 mM. The increased inhibition effectiveness is because more DMAPAAP molecules bind to the mild steel surface and create a protective layer [34]. However, as the DMAPAAP concentration exceeds 0.5 mM, the molecules start to desorb from the mild steel surface, reducing the effectiveness of the protection.

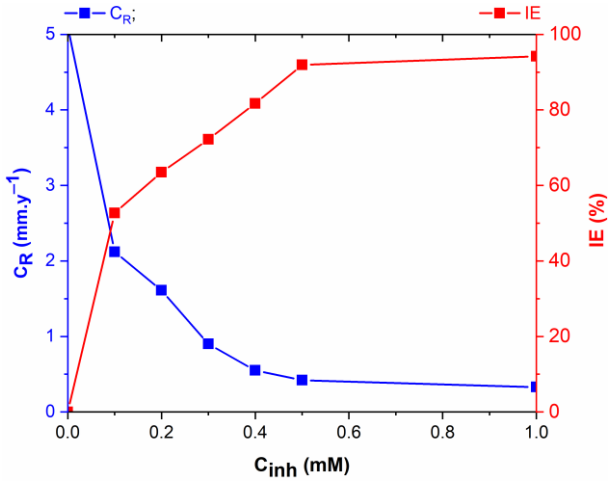

Figure 2: The comparison between corrosion and inhibition effectiveness rates in uninhibited and inhibited HCl solutions after 5 hours of immersion time at 303 K.

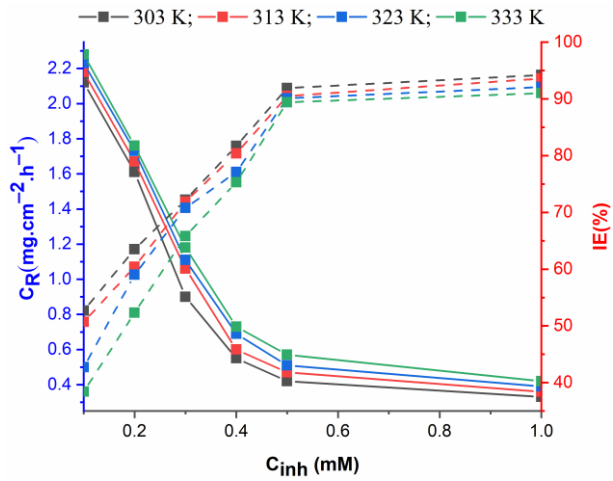

Figure 4: Comparison between the corrosion rate and inhibition efficiency in inhibited 1 M HCl with different doses of DMAPAAP, at the temperature 303–333 K for 5 h exposure period.

3.2. Exposure periods effect

The impact of exposure duration on the inhibition efficiency of a corrosion inhibitor for metallic substrate corrosion in a corrosive solution was investigated by immersing the metallic substrate in an inhibited hydrochloric acid solution with different inhibitor concentrations for various immersion periods (1, 5, 10, 24, and 48 hours) at 303 K. The results, illustrated in Figure 3, show that the inhibition efficiency increases significantly with increasing immersion duration of up to 5 hours and then gradually with longer exposure times of up to 24 hours. After 24 hours, the protective performance begins to decline, and after 48 hours, it eventually stabilizes. This increase in inhibition efficiency is attributed to the larger number of inhibitor molecules attaching to the mild steel surface with longer exposure times, forming a protective layer [35]. As more DMAPAAP molecules adsorb onto the metallic substrate, the adsorption intensity improves, allowing the van der Waals force to interact with the inhibitor molecules. Although some inhibitor molecules may leave the surface, reducing the active area that the inhibitor covers and its effectiveness, the high inhibition efficiency observed during a longer exposure duration demonstrates the stability of the adsorbed inhibitor layer in the corrosive solution [36].

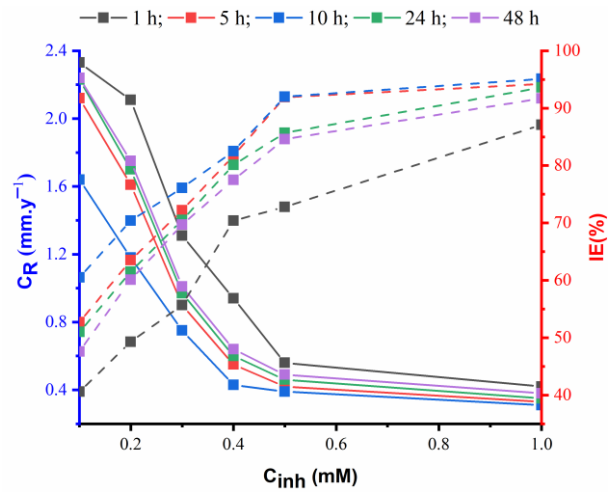

Figure 3: The effect of immersion time on the inhibition efficiency of a corrosion inhibitor for metallic substrate corrosion in 1 M HCl at 303K.

3.3. Temperature effects

Weight loss experiments were conducted at different temperatures (303, 313, 323, and 333 K) to examine the impact of temperature on the corrosion inhibition properties of DMAPAAP, and the activation variables were calculated [37]. As shown in Figure 4, which presents the effect of temperature on the corrosion rate of the metallic substrate in both uninhibited and inhibited solutions at the optimum inhibitor concentration in a 1 M HCl acidic environment, it can be observed that the corrosion rates slightly increase with temperature for a given inhibitor concentration. This observation can be attributed to the increased thermal agitation of DMAPAAP particles in the corrosive environment at higher temperatures, leading to higher conductivity and acidic activity of the solution. Consequently, the inhibition efficiency decreases as the

temperature rises, increasing the corrosion rate (38). The data obtained from the experiments support this trend. For instance, at 303 K in a 1 M HCl medium, the inhibition efficiency reached 91.8 % in the presence of the tested 0.5 mM inhibitor. It is worth noting that this inhibitor concentration has not been previously reported and represents a novel inhibitor suitable for hydrochloric acid solutions.

Furthermore, the performance of the inhibitor surpassed that of previously published inhibitors, indicating that an effective inhibitor in corrosive media must maintain its protective performance even at high temperatures. This aspect is particularly important in industries such as the petroleum sector, where downhole temperatures are typically elevated [39]. By including this discussion, we aim to provide a more comprehensive understanding of the relationship between temperature, corrosion rates, and the inhibitory properties of DMAPAAP. This information highlights the practical significance of our findings and their potential applications in industries where high-temperature corrosion is a critical concern.

3.4. Adsorption isotherm

Inhibition of corrosion by chemical inhibitors is caused by the adsorption of inhibitor molecules onto the metal surface. Understanding the adsorption process is important for determining the inhibition mechanism of the inhibitor. To identify the adsorption process, three adsorption isotherms - Frumkin, Temkin, and Langmuir - were studied, and the percentage of surface coverage was calculated. The Langmuir isotherm was the most appropriate option among the analyzed isotherms, as it showed a straight line with a regression coefficient R^2 value close to unity (Figure 5). The slope value for the tested inhibitor was also close to unity, confirming the validity of the Langmuir isotherm. The Langmuir adsorption isotherm is often represented by equation 11 [40].

$$C_{inh}/\theta = (K_{ads})^{-1} + C \quad (11)$$

where K_{ads} is the adsorption constant, and θ is the surface coverage.

Figure 5 provides important information on the K_{ads} value for the tested inhibitor, which is summarized in Table 1. A larger K_{ads} value indicates stronger adsorption of inhibitor molecules onto the surface of mild steel, indicating better corrosion inhibition performance [41]. According to Table 1, the tested inhibitor has the highest K_{ads} value, indicating the highest adsorption on the mild steel surface. Using the relationship [42], K_{ads} values can be used to calculate the standard free energy of adsorption (ΔG^o_{ads}) using equation 12.

$$\Delta G^o_{ads} = -RT \ln(55.5 K_{ads}) \quad (12)$$

The negative value of 0 ΔG^o_{ads} suggests a spontaneous adsorption process, resulting in a stable layer of inhibitor molecules on the mild steel surface. Physical adsorption involves Van der Waals forces between inhibitor molecules and the metallic substrate, typically resulting in ΔG^o_{ads} values less than –20 kJ.mole^{-1}. On the other hand, values more negative than –40 kJ·mole^{-1} involve the transfer of unpaired electrons of heteroatoms in the inhibitor molecules to the d-orbitals of iron atoms located on the metallic surface, forming coordination bonds, known as chemisorption [43]. In the current study, ΔG^o_{ads} values range from –29.7 to –34.0 kJ. mole^{-1}, suggesting the occurrence of both physisorption and chemisorption mechanisms. Chemisorbed molecules are expected to provide better protection by reducing the metal's reactivity at the linked spots. Distinguishing chemisorption and physisorption is difficult when only ΔG^o_{ads} values are considered because they can have some overlap. Physical adsorption occurs before chemical adsorption, which is also widely accepted [44].

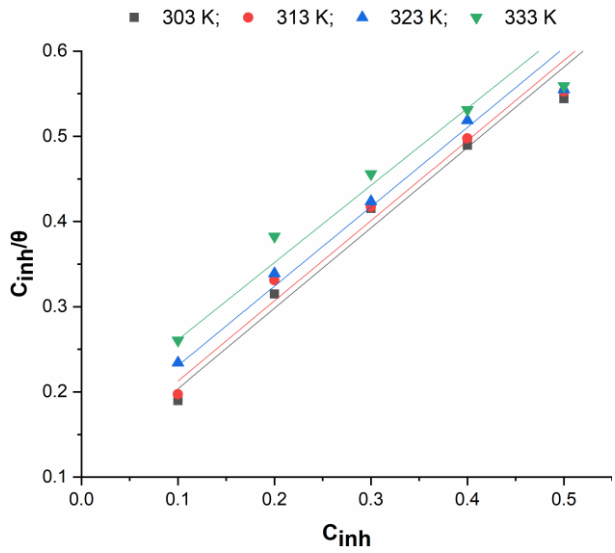

Figure 5: Langmuir adsorption isotherm.

Table 1: The thermodynamic parameters which computed based on weight loss measurements ant different temperatures.

Parameters	303 K	313 K	323 K	333 K
Intercept	0.109 ± 0.01	0.118 ± 0.0	0.137 ± 0.01	0.170 ± 0.02
Slope	0.943 ± 0.03	0.940 ± 0.03	0.93 ± 0.03	0.905 ± 0.05
R-Square	0.994	0.994	0.99	0.986

3.5. DFT

The quantum chemical technique can provide valuable information on the structural characteristics of DMAPAAP molecules, including various thermodynamic parameters. Gaussian records at B3LYP/6-311G (d,p) can be used to determine such parameters based on the structural parameters of DMAPAAP, as illustrated in Figure 6.

To identify inhibitor adsorption sites, Mulliken charges are commonly utilized. According to Figure 7, the oxygen and nitrogen atoms in DMAPAAP with negative charges are the preferred adsorption locations for this inhibitor due to their donor-acceptor interactions with metal surfaces.

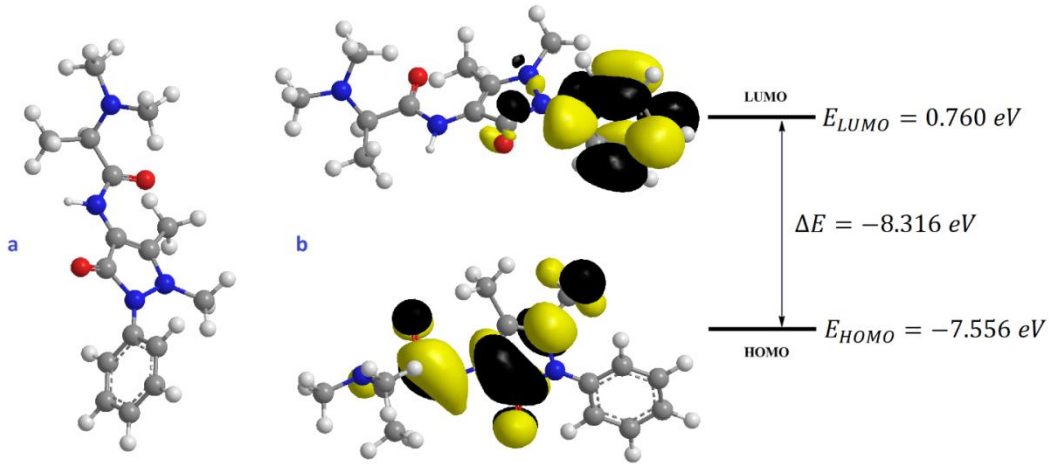

Figure 6: (a) Optimized structure and (b) Energy gap plot of DMAPAAP.

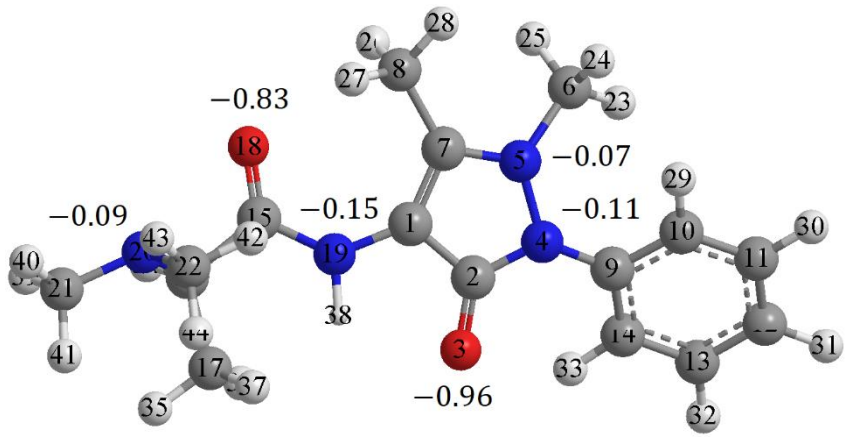

Figure 7: Mulliken charges of DMAPAAP.

Table 2: DFT variables for DMAPAAP molecules in the gas phase.

I (eV)	A (eV)	E_{HOMO} (eV)	E_{LUMO} (eV)	ΔE (eV)	χ (eV)	η (eV)	σ (eV^{-1})	ΔN (eV)
7.556	0.760	-7.556	0.760	-8.316	4.158	3.398	0.294	0.418

The benzene ring in DMAPAAP molecules also facilitates the formation of complexations between adsorbate and surface coordination bonds. The highest occupied molecular orbital (HOMO) can indicate the site for electron donation in the molecule [45]. For DMAPAAP, the HOMO in Figure 7 indicates that the O and N atoms can transfer electrons to the metallic substrate. On the other hand, the lowest unoccupied molecular orbital (LUMO) indicates the molecule's capability to accept electrons [46]. Figure 7 reveals that the DMAPAAP reception sites are equivalent and that the most reactive LUMO locations in DMAPAAP are the N, O, and C atoms.

Table 2 presents the quantum chemical parameters determined through computations, including E_{HOMO}, E_{LUMO}, ΔE, electronegativity (χ), softness (σ), hardness (η), and the number of electrons transported (ΔN). A molecule with a higher E_{HOMO} value can donate electrons more easily, whereas a smaller E_{LUMO} value indicates a molecule's ability to accept electrons. The absolute hardness (η) measures the molecule's stability, whereas global softness (σ) indicates the electron cloud polarization in composites. A good corrosion inhibitor should have low values of ΔE but high values of σ. DMAPAAP has a low E_{HOMO} value indicates its ability to donate electrons, and high ΔN value indicates better electron exchange ability. The calculated values in Table 2 indicate that DMAPAAP is an effective corrosion inhibitor, and there is good agreement between the test results and quantitative chemical parameters (E_{LUMO}, E_{HOMO}, ΔE, η, σ, and ΔN). When a metal shares electrons with the inhibitor (back donation), it establishes contact between the metal surfaces and the inhibitor.

3.6. Suggested mechanism

Organic inhibitor molecules bind to steel surfaces to initiate their inhibitory effect. The inhibitor's chemical nature, metal type, charged surface, and charge distribution throughout the inhibitor molecule influence the adsorption mechanism. There are different methods by which organic inhibitors can adhere to metallic substrates, including electrostatic interaction, unshared electron pairs interaction, p-electron interaction, or a combination of all three. For DMAPAAP, the oxygen and nitrogen atoms, heterocyclic, and benzene rings play a role in their high inhibitory effectiveness, with the unpaired electron pairs of these atoms being potential coordinating centers. In acidic environments, DMAPAAP is present as protonated molecules on uncharged particles [45-47]. The adsorption mechanism of inhibitor particles on the metallic surface may involve various methods, such as interactions between donors and acceptors of π-bonds and unoccupied iron d-orbitals, electrostatic interactions, and interactions between unoccupied iron d-orbitals and unpaired electrons of nitrogen and oxygen atoms. It is challenging for positive ion particles in corrosive solutions to reach positively charged mild steel surfaces, but protonated inhibitor molecules can be adsorbed through electrostatic interactions. Inhibitor ions (protonated inhibitor molecules) interact with negatively charged chloride ions on steel surfaces to cause the hydration of chlorides and favor the inhibitor ions' positive charge. However, a single adsorption mechanism cannot explain the adsorption process of inhibitor molecules on metallic substrates in corrosive environments [48-51]. As shown in Figure 8, different methods may be used to demonstrate the adsorption mechanism process.

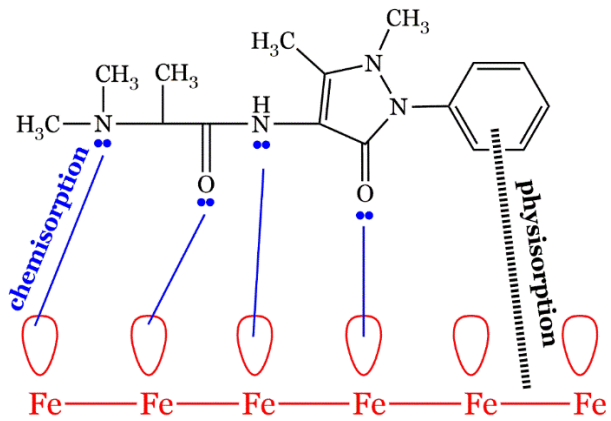

Figure 8: Postulated inhibition mechanism.

4. Conclusion

In conclusion, this study demonstrates that 2-dimethylaminopropionamidoantipyrine (DMAPAAP) can be used as an effective corrosion inhibitor for mild steel in hydrochloric acid (HCl) solution. The corrosion inhibition efficiency of DMAPAAP was found to increase with increasing electron-donating groups in the molecule, resulting in the formation of a protective film on the metal surface. The Langmuir adsorption isotherm was the most suitable model to describe the adsorption behavior of DMAPAAP on the mild steel surface. The experimental results were supported by density functional theory (DFT) calculations, providing a deeper understanding of the inhibition mechanism of DMAPAAP. Overall, the combined experimental and theoretical study provides valuable insights into the potential use of DMAPAAP as a corrosion inhibitor for mild steel in industrial applications. Further research can explore the effectiveness of DMAPAAP under different experimental conditions and investigate its performance in more aggressive acidic environments.

5. References

1. Aljibori HS, Abdulzahra OH, Al-Adily AJ, Al-Azzawi WK, Al-Amiery A., Kadhum AAH. Corrosion inhibition effects of concentration of 2-oxo-3-hydrazonoindoline in acidic solution, exposure period, and temperature. Int J Corr Scale Inhib. 2023; 12(2): 438-457. https://doi.org/10.17675/2305-6894-2023-12-2-4.
2. Junaedi S, Kadhum AAH, Al-Amiery A, Mohamad AB, Takriff MS. Synthesis and characterization of novel corrosion inhibitor derived from oleic acid: 2-Amino-5- Oleyl 1,3,4-Thiadiazol (AOT). Int J Electrochem Sci. 2012; 7(4): 3543-3554.
3. Aljibori HS, Alwazir AH, Abdulhadi S, Al-Azzawi WK, Kadhum AAH, Shaker LM, Al-Amiery AA, Majdi HSh. The use of a Schiff base derivative to inhibit mild steel corrosion in 1 M HCl solution: a comparison of practical and theoretical findings. Int J Corr Scale Inhib., 2022, 11(2): 1435–1455.
4. Al-Azzawi WK, Salih SM, Hamood A., Al-Azzawi RK, Kzar MH, Jawoosh HN, Shakier LM, Al-Amiery A, Kadhum AAH, Isahak WNRW, Takriff MS. Adsorption and theoretical investigations of a Schiff base for corrosion inhibition of mild steel in an acidic environment. Int J Corr Scale Inhib., 2022; 11(2), 1063-1082.
5. Jamil DM, Al-Okbi A, Hanon M, Rida KS, Alkaim A, Al-Amiery A, Kadhum A, Kadhum AAH. Carbethoxythiazole corrosion inhibitor: as an experimentally model and DFT theory. J Eng Appl Sci. 2018; 13(11): 3952-3959.
6. Alobaidy A, Kadhum A, Al-Baghdadi S, Al-Amiery A, Kadhum A, Yousif E, Mohamad AB. Eco-friendly corrosion inhibitor: experimental studies on the corrosion inhibition performance of creatinine for mild steel in HCl complemented with quantum chemical calculations. Int J Electrochem Sci. 2015; 10(3):3961-3972.
7. Alamiery AA. Study of corrosion behavior of N´-(2-(2-oxomethylpyrrol-1-yl) ethyl)piperidine for mild steel in the acid environment. Biointerface Res Appl Chem. 2022; 12(3): 3638-3646.
8. Alamiery A, Mohamad AB, Kadhum AAH, Takriff MS. Comparative data on corrosion protection of mild steel in HCl using two new thiazoles. Data Brief. 2022; 40: 107838. https://doi.org/10.1016/j.dib.2022.107838
9. Mustafa AM, Sayyid FF, Betti N, Shaker LM, Hanoon MM, Alamiery AA, Kadhum AAH, Takriff MS. Inhibition of mild steel corrosion in hydrochloric acid environment by 1-amino-2-mercapto-5-(4-(pyrrol-1-yl)phenyl)-1,3,4-triazole. S. Afr. J Chem Eng. 2022; 39(4):42-51.https://doi.org/10.1016/j.sajce.2021.11.009.
10. Alamiery AA. Investigations on corrosion inhibitory effect of newly quinoline derivative on mild steel in HCl solution complemented with antibacterial studies. Biointerface Res Appl Chem. 2022; 12(4): 1561-1568.
11. Aziz IAA, Annon IA, Abdulkareem MH, Hanoon MM, Alkaabi MH, Shaker LM, Alamiery AA, Isahak WNRW, Takriff MS. Insights into corrosion inhibition behavior of a 5-mercapto-1, 2, 4-triazole derivative for mild steel in hydrochloric acid solution: experimental and DFT studies. Lubricants. 2021; 9(12): 122. https://doi.org/10.3390/lubricants9120122.
12. Alamiery A. Short report of mild steel corrosion in 0.5 M H_2SO_4 by 4-ethyl-1-(4-oxo4-phenylbutanoyl) thiosemicarbazide. J Tribologi. 2021; 30: 90-99.
13. Alamiery AA, Isahak WNRW, Takriff MS. Inhibition of mild steel corrosion by 4-benzyl-1-(4-oxo-4-phenylbutanoyl)thiosemicarbazide: Gravimetrical, adsorption and theoretical studies. Lubricants. 2021; 9(9): 93. https://doi.org/10.3390/lubricants9090093.
14. Dawood MA, Alasady ZMK, Abdulazeez MS, Ahmed DS, Sulaiman GM, Kadhum AAH, Shaker LM, Alamiery AA. The corrosion inhibition effect of a pyridine derivative for low carbon steel in 1 M HCl medium: Complemented with antibacterial studies. Int J Corr Scale Inhib. 2021; 10(5): 1766-1782.
15. Alamiery A. Corrosion inhibition effect of 2-N-phenylamino-5-(3-phenyl-3-oxo-1- propyl)-1,3,4-oxadiazole on mild steel in 1 M hydrochloric acid medium: Insight from gravimetric and DFT investigations. Mater Sci Energy Technol. 2021; 4: 398-406. https://doi.org/10.1016/j.mset.2021.09.002

16. Alamiery AA. Anticorrosion effect of thiosemicarbazide derivative on mild steel in 1 M hydrochloric acid and 0.5 M sulfuric Acid: Gravimetrical and theoretical studies. Mater Sci Energy Technol. 2021; 4: 263-273. https://doi.org/10.1016/j.mset.2021.07.004.
17. Alamiery AA, Isahak WNRW, Aljibori HSS, Al-Asadi HA, Kadhum AAH. Effect of the structure, immersion time and temperature on the corrosion inhibition of 4-pyrrol-1-yln-(2,5-dimethyl-pyrrol-1-yl)benzoylamine in 1.0 M HCl solution. Int J Corr Scale Inhib., 2021; 10(6): 700-713. https://doi.org/10.17675/2305-6894-2021-10-2-14.
18. Alamiery A, Mahmoudi E, Allami T. Corrosion inhibition of low-carbon steel in hydrochloric acid environment using a Schiff base derived from pyrrole: gravimetric and computational studies. Int J Corr Scale Inhib. 2021; 10(4): 749-765.
19. Eltmimi AJM, Alamiery A, Allami AJ, Yusop RM, Kadhum A., Allami T. Inhibitive effects of a novel efficient Schiff base on mild steel in hydrochloric acid environment. Int J Corr Scale Inhib. 2021; 10(3): 634-648.
20. Alamiery A, Shaker LM, Allami T, Kadhum AH, Takriff MS. A study of acidic corrosion behavior of furan-derived schiff base for mild steel in hydrochloric acid environment: Experimental, and surface investigation. Mater Today: Proc. 2021; 44(6): 2337-2341.
21. Mahdi BS, Aljibori HSS, Abbass M., Al-Azzawi WK, Kadhum AH, Hanoon MM, Isahak WNRW, Al-Amiery AA, Majdi HSh. Gravimetric analysis and quantum chemical assessment of 4-aminoantipyrine derivatives as corrosion inhibitors, Int J Corr Scale Inhib. 2022; 11(9): 1191-1213.
22. Junaedi S, Al-Amiery AA, Kadihum A, Kadhum AAH, Mohamad AB. Inhibition effects of a synthesized novel 4-aminoantipyrine derivative on the corrosion of mild steel in hydrochloric acid solution together with quantum chemicalstudies. Int J Mol Sci. 2013; 14(6): 11915-11928. https://doi.org/10.3390/ijms140611915
23. Al-Baghdadi SB, Al-Amiery AA, Gaaz TS, Kadhum AAH. Terephthalohydrazide and isophthalohydrazide as new corrosion inhibitors for mild steel in hydrochloric acid: Experimental and theoretical approaches. Koroze Ochr Mater. 2021; 65(8): 12-22.
24. Al-Baghdadi S, Gaaz TS, Al-Adili A, Al-Amiery AA, Takriff MS. Experimental studies on corrosion inhibition performance of acetylthiophene thiosemicarbazone for mild steel in HCl complemented with DFT investigation. Int J Low-Carbon Technol. 2021; 16(6): 181-188. https://doi.org/10.1093/ijlct/ctaa050.
25. ASTM International, Standard Practice for Preparing, Cleaning, and Evaluating Corrosion Test, 2011, 1–9.
26. NACE International, Laboratory Corrosion Testing of Metals in Static Chemical Cleaning Solutions at Temperatures below 93°C (200°F), TM0193-2016-SG, 2000.
27. Hanoon MM, Resen AM, Shaker LM, Kadhum AAH, Al-Amiery AA. Corrosion investigation of mild steel in aqueous hydrochloric acid environment using N-(naphthalen-1yl)-1-(4-pyridinyl)methanimine complemented with antibacterial studies. Biointerface Res.Appl Chem. 2021; 11(6): 9735-9743.
28. Al-Amiery AA. Anti-corrosion performance of 2-isonicotinoyl-Nphenylhydrazinecarbothioamide for mild steel hydrochloric acid solution: Insights from experimental measurements and quantum chemical calculations. Surf Rev Lett. 2021; 28(3): 2050058. https://doi.org/10.1142/S0218625X20500584.
29. Abdulazeez MS, Abdullahe ZS, Dawood MA, Handel ZK, Mahmood RI, Osamah S, Kadhum AH, Shaker LM, Al-Amiery AA. Corrosion inhibition of low carbon steel in HCl medium using a thiadiazole derivative: weight loss, DFT studies and antibacterial studies. Int J Corr Scale Inhib. 2021; 10(6): 1812-1828.
30. Mustafa AM, Sayyid FF, Betti N, Hanoon MM, Al-Amiery A, Kadhum AAH, Takriff MS. Inhibition evaluation of 5-(4-(1H-pyrrol-1-yl)phenyl)-2-mercapto1,3,4-oxadiazole for the corrosion of mild steel in an acid environment: thermodynamic and DFT aspects. Tribologia. 2021; 38(4): 39-47. https://doi.org/10.30678/FJT.105330.
31. Abdulsahib YM, Eltmimi AJM, Alhabeeb SA, Hanoon MM, Al-Amiery AA, Allami T, Kadhum AAH. Experimental and theoretical investigations on the inhibition efficiency of N-(2,4-dihydroxytoluen-eylidene)-4-methylpyridin-2-amine for the corrosion of mild steel in hydrochloric acid. Int J Corr Scale Inhib. 2021; 10(6): 885-899.
32. Frisch MJ, Trucks GW, Schlegel HB, Scuseria GE, Robb MA, Cheeseman JR, Montgomery JA, Vreven T, Kudin KN, Burant JC, Millam JM, Iyengar SS, Tomasi J, Barone V, Mennucci B, Cossi M, Scalmani G, Rega N, Petersson GA, Nakatsuji H, Hada M, Ehara M, Toyota K, Fukuda R, Hasegawa J, Ishida M, Nakajima T, Honda Y, Kitao O, Nakai H, Klene M, Li X, Knox JE, Hratchian HP, Cross JB, Bakken V, Adamo C, Jaramillo J, Gomperts R, Stratmann RE, Yazyev O, Austin AJ, Cammi R, Pomelli C, Ochterski JW, Ayala PY, Morokuma K, Voth GA, Salvador P, Dannenberg JJ, Zakrzewski VG, Dapprich S, Daniels AD, Strain MC, Farkas O, Malick DK, Rabuck AD, Raghavachari K, Foresman JB, Ortiz JV, Cui Q, Baboul AG, Clifford S, Cioslowski J, Stefanov BB, Liu G, Liashenko A, Piskorz P, Komaromi I, Martin RL, Fox DJ, Keith T, Al-Laham MA, Peng CY, Nanayakkara A, Challacombe M, Gill PMW, Johnson B., Chen W, Wong MW, Gonzalez C, Pople JA. Gaussian 03, Revision B. 05, Gaussian, Inc., Wallingford, CT, 2004.
33. Koopmans T. Ordering of wave functions and eigen-energies to the individual electrons of an atom. Physica. 1934; 1(4): 104-113 (In German).
34. Khudhair AK, Mustafa AM, Hanoon MM, Al-Amiery A, Shaker LM, Gazz T, Mohamad AB, Kadhum AH, Takriff MS. Experimental and theoretical investigation on the corrosion inhibitor potential of N-MEH for mild

steel in HCl. Prog Color Colorant Coat. 2022; 15(2): 111-122. https://doi.org/10.30509/pccc.2021.166815.1111.
35. Zinad DS, Salim RD, Betti N, Shaker LM, AL-Amiery AA. Comparative investigations of the corrosion inhibition efficiency of a 1-phenyl-2-(1-phenylethylidene)hydrazine and its analog against mild steel corrosion in hydrochloric acid solution. Prog Color Colorant Coat. 2022; 15(1), 53-63. https://doi.org/10.30509/pccc.2021.166786.1108
36. Salim RD, Betti N, Hanoon M, Al-Amiery AA. 2-(2,4-Dimethoxybenzylidene)- N-phenylhydrazinecarbothio-amide as an efficient corrosion inhibitor for mild steel in acidic environment. Prog Color Colorant Coat. 2021; 15(1): 45-52. https://doi.org/10.30509/pccc.2021.166775.1105.
37. Al-Amiery AA, Shaker LM, Kadhum AH, Takriff MS. Exploration of furan derivative for application as corrosion inhibitor for mild steel in hydrochloric acid solution: Effect of immersion time and temperature on efficiency. Mater Today: Proc. 2021; 42(6): 2968–2973.
38. Resen AM, Hanoon MM, Alani WK, Kadhim A, Mohammed AA, Gaaz TS, Kadhum AAH, Al-Amiery AA, Takriff MS. Exploration of 8-piperazine-1-ylmethylumbelliferone for application as a corrosion inhibitor for mild steel in hydrochloric acid solution. Int J Corr Scale Inhib. 2021, 10(2):, 368-387.
39. Hanoon MM, Resen AM, Al-Amiery AA, Kadhum AAH, Takriff MS. Theoretical and experimental studies on the corrosion inhibition potentials of 2-((6- methyl-2-ketoquinolin-3-yl)methylene) hydrazinecarbothioamide for mild steel in 1 M HCl. Prog Color Colorant Coat. 2022; 15(1): 11-23. https://doi.org/10.30509/pccc.2020.166739.1095.
40. Hashim FG, Salman TA, Al-Baghdadi SB, Gaaz T, Al-Amiery AA. Inhibition effect of hydrazine-derived coumarin on a mild steel surface in hydrochloric acid. Tribologia. 2020; 37(3): 45-53. https://doi.org/10.30678/FJT.95510.
41. Resen AM, Hanoon M, Salim RD, Al-Amiery AA, Shaker LM, Kadhum AAH. Gravimetrical, theoretical investigations, and surface morphological investigations of corrosion inhibition effect of 4-(benzoimidazole-2-yl)pyridine on mild steel in hydrochloric acid. Koroze Ochr Mater. 2020; 64(1): 122-130. https://doi.org/10.2478/kom-2020-0018
42. Salman AZ, Jawad QA, Ridah KS, Shaker LM, Al-Amiery AA. Selected bisthiadiazole: synthesis and corrosion inhibition studies on mild steel in HCl environment. Surf Rev Lett. 2020; 27(3): 2050014.
43. Alamiery AA, Isahak WNRW, Aljibori HSS, Al-Asadi HA, Kadhum AAH. Effect of the structure, immersion time and temperature on the corrosion inhibition of 4-pyrrol-1-yl-N-(2,5-dimethyl-pyrrol-1-yl)benzoylamine in 1.0 M HCl solution. Int J Corr Scale Inhib. 2021; 10(5): 700-713.
44. Al-Baghdadi SB, Hashim FG, Salam AQ, Abed TK, Gaaz TS, Al-Amiery AA, Kadhum AAH, Reda KS, Ahmed WK. Synthesis and corrosion inhibition application of NATN on mild steel surface in acidic media complemented with DFT studies. Results Phys. 2018; 8(6): 1178-1184.
45. Al-Azzawi WK, Al Adily AJ, Sayyid FF, Al-Azzawi RK, Kzar MH, Jawoosh HN, Al-Amiery AA, Kadhum AAH, Isahak WNRW, Takriff MS. Evaluation of corrosion inhibition characteristics of an N-propionanilide derivative for mild steel in 1 M HCl: Gravimetrical and computational studies. Int J Corr Scale Inhib. 2022; 11(3): 1100-1114.
46. Al-Edan AK, Isahak WNRW, Ramli ZAC, Al-Azzawi WK, Kadhum AAH, Jabbar HS, Al-Amiery A. Palmitic acid-based amide as a corrosion inhibitor for mild steel in 1M HCl. Heliyon. 2023; 9(4), e14657. https://doi.org/10.1016/j.heliyon.2023.e14657
47. Sayyid FF, Mustafa AM, Hanoon MM, Saker LM, Alamiery AA. Corrosion protection effectiveness and adsorption performance of schiff base-quinazoline on mild steel in HCl environment. Corros Sci Tech. 2022; 21(4): 77-88.
48. Al-Amiery AA, Mohamad AB, Kadhum AAH. Experimental and theoretical study on the corrosion inhibition of mild steel by nonanedioic acid derivative in hydrochloric acid solution. Sci Rep. 2022; 12(6): 4705. https://doi.org/10.1038/s41598-022-08146-8.
49. Al-Amiery AA, Al-Azzawi WK, Isahak WNRW. Isatin Schiff base is an effective corrosion inhibitor for mild steel in hydrochloric acid solution: gravimetrical, electrochemical, and computational investigation. Sci Rep. 2022; 12(4): 17773. https://doi.org/10.1038/s41598-022-22611-4.
50. Al-Amiery A, Isahak WNRW, Al-Azzawi WK. Multi-method evaluation of a 2-(1,3,4-thiadiazole-2-yl)pyrrolidine corrosion inhibitor for mild steel in HCl: combining gravimetric, electrochemical, and DFT approaches. Sci Rep. 2023; 13(4): 9770. https://doi.org/10.1038/s41598-023-36252-8.
51. Al-Amiery A, Binti Kassim F, Kadhum A. Synthesis and characterization of a novel eco-friendly corrosion inhibition for mild steel in 1 M hydrochloric acid. Sci Rep. 2016;6(3):19890. https://doi.org/10.1038/srep19890.

How to cite this article:
Abbass MK, Raheef KM, Aziz IA, Hanoon MM, Mustafa AM, Al-Azzawi WK, Al-Amiery AA, Kadhum AAH. Evaluation of 2-Dimethylaminopropionamidoantipyrine as a Corrosion Inhibitor for Mild Steel in HCl Solution: A Combined Experimental and Theoretical Study. Prog Color Colorants Coat. 2024;17(1):1-10. Doi: 10.30509/pccc.2023.167081.1197.